Analysis of continuous snow temperature profiles from automatic weather stations in Aosta Valley (NW Italy): Uncertainties and applications

ANALYSIS OF CONTINUOUS SNOW TEMPERATURE PROFILES FROM AUTOMATIC WEATHER STATIONS IN AOSTA VALLEY (NW ITALY): UNCERTAINTIES AND APPLICATIONS

G. Filippa, M. Maggioni, E. Zanini, M. Freppaz

Gianluca Filippa, Dipartimento di Scienze Agrarie, Forestali e Alimentari and NatRisk-LNSA, University of Torino, Via L. Da Vinci 44, 10095 Grugliasco (TO), Italy; tel. +39 011 6708522, fax.+39 011 6708692; email: gianluca.filippa@unito.it

Abstract

Continuous measurements of snow temperature profiles may be a valuable tool to investigate occurrence and persistence of thermal conditions promoting strengthening or weakening of the snow structure, with potentially important consequences on avalanche release. In this paper, automatic measurements of snow temperature profiles are analysed based on an extensive dataset (67 site-years) in Aosta Valley, Italy. The aims of this work are: (1) to highlight issues and uncertainties on the data and show appropriate data filtering that may be implemented by similar measurement networks; (2) to assess the impact of data filtering on temperature gradient calculation and, (3) to quantitatively describe the occurrence and duration of strong temperature gradients at the base of the snowpack and close to the snow surface that may lead to snowpack instability.

Three main sources of uncertainty were identified and corrected: (1) errors in the data logging; (2) drifts in temperature measurements; (3) a large bias

in spring measurements due to snow melting and lack of contact between the sensor and the surrounding snow.

We estimated that strong temperature gradients may account for as much as 25% of total gradients and the duration of these may be as long as 35 days. The frequency of strong gradients was significantly higher at the snow surface than at the snowpack base. Hence, it is highlighted the importance of surface faceted crystals as potential weak layers in alpine snowpacks.

Keywords: data filtering, snow temperature gradient, depth hoar, near-surface faceted crystals, snowpack instability, snow/soil interface

---

1. Introduction

Temperature distribution in the snowpack is a consequence of the snow-atmosphere interactions at the surface and of ground heat fluxes at the lower boundary (or base) of the snowpack. Hence, snow temperatures are strictly related to the energy balance of the snowpack and are commonly used to calculate temperature gradients. In turn, temperature gradients are responsible for the snow metamorphism which can lead the snowpack towards stability or instability conditions. After depositing on the ground, the seasonal snow cover continues to change due to differences in vapor pressure within the ice lattice. It is primarily the temperature gradient, along with the snow structure, that drives differences in vapor pressure resulting in crystal metamorphism. In particular, the metamorphism is of interest because it can indicate strengthening or weakening of the grain structure (Shea et al., 2012).

Therefore, it is common among the Avalanche Warning Services to periodically measure, beside other physical properties, the snow temperature profile

in specific locations, in order to predict the possible evolution of snowpack structure.

In some cases, snow temperatures are continuously registered from automatic weather stations (AWS) or are calculated by models, which are able to describe the snowpack structure on the basis of only few snow and meteorological data, such as for example air temperature, solar radiation, and surface snow temperature (Brun et al., 1989; Morland et al., 1990; Jordan et al., 1991; Lehning et al., 1999).

When using data from manual snow profiles, the temperature gradient of the entire snowpack is calculated considering the snow surface temperature, the ground surface temperature and the snow depth. However, surface snow temperature varies greatly during the day (Fierz, 2011). Diurnal temperature fluctuation within the top portion of the snowpack is the result of the net energy balance at the snow surface, which includes different contributions. Among them the most relevant are the radiation fluxes: short wave radiation flux and net long wave radiation flux (Gray and Male, 1981). McClung and Sharer (2006) suggested that short wave radiations can penetrate within the snowpack to a depth of 10-20 cm. Higher values were reported by Fierz (2011) and Ohara and Kavvas (2006): the thickness of what they call active layer, where the snow temperature shows diurnal variation, reached about 50 and 60 cm, respectively. However, the depth of short wave penetration is strictly related to the properties of the surface snowpack layers (Bakermans et al., 2006).

Birkeland (1998) reports that the temperature 0.30 m below the surface changes little, if at all, on a daily basis, and represents a sort of diurnal

average. The temperature difference between the cooling and warming snow surface and the relatively consistent temperature at 0.30 m below the snow surface results in strong temperature gradients in the near-surface layers which might lead to the formation of near-surface faceted crystals.

At the other end of the snowpack, close to the ground surface, kinetic metamorphism is promoted by the high vapor pressure, as snow temperatures are generally close to 0 °C, with the formation of depth hoar (Giddings and LaChapelle, 1962; Colbeck, 1983).

Moreover, within the snowpack, conditions favorable to the growth of faceted crystals can be present, especially close to ice crusts (Colbeck and Jamieson, 2001; Adams and Brown , 1983). Laboratory experiments by Greene et al. (2006) have shown that, under a constant uni-directional strong temperature gradient, increased bonding and greater mechanical strength occur on the warm side of the ice lense while the cold side stay or become weak. Depending on the orientation of the temperature gradient, the weak layer can be on the top or on the bottom of the crust.

Hence, the study of partial gradients, even if measured at relatively coarse stratigraphic scale (i.e. 20 cm increments), may give insight on local occurrence of conditions that could promote snowpack instability. Near-surface faceted crystals and depth hoar are examples of temperature-gradient metamorphism near the surface or extending down through the base of the snowpack. For example, Birkeland (1998) found that 59% of avalanches released on faceted crystals formed near the surface before being subsequently buried. Not only the strength of the gradient is important to the formation of weak layers, but also its duration plays a key role. In a recent study, Marienthal et

al. (2012) found that different avalanche cycles occurred on depth hoar during the 2012 winter in south-west Montana. Schweizer and Jamieson (2001) reported that 70% of 186 skier-triggered avalanches were released due to weak layers of persistent grain types (i.e. surface hoar, faceted crystals, and depth hoar).

Mechanisms and processes affecting thermal properties of snow are well described in literature (Gray and Male, 1981; Jones et al., 2001; Kaempfer et al., 2005; Fierz, 2011) and it is not among the objectives of this paper to add new findings on this topics. Instead, we analyzed an existing extensive dataset (67 site-years) of continuous snow temperature profiles at 6 sites in Aosta Valley, NW-Italy, in order to:
(1) highlight issues and uncertainties on the data and show appropriate data filtering that may be implemented by similar measurement networks,
(2) calculate snow temperature gradient and assess the impact of data filtering on gradient calculation, and
(3) quantitatively describe the occurrence and duration of strong temperature gradients at the base of the snowpack and close to the snow surface that may promote snowpack instability.

2. Materials and methods

2.1. Study Area

Automatic weather stations (AWS) used in this study are located in the North-western portion of Aosta Valley (Fig.1, table 1). Aosta Valley surface area is 3262 km^2, the mean altitude is 2106 m a.s.l., with more than 80%

of its territory above 1500 m a.s.l.. Mean annual air temperature (T_{air}) at 2000 m a.s.l. ranges from -0.2 to 3.1 °C. The climate of the region is strongly affected by the presence of surrounding high mountains, resulting in a typical inner alpine continental climate (Mercalli et al., 2003). Topography in this region exerts a major influence on several meteorological variables, as for example on the precipitation: while on the south-eastern boundary of the region the external mountain side receives as much as 2000 mm y^{-1}, about 70% of the region receives less than 1000 mm y^{-1} precipitation with minima of less than 500 mm in the most inner part (Mercalli et al., 2003).

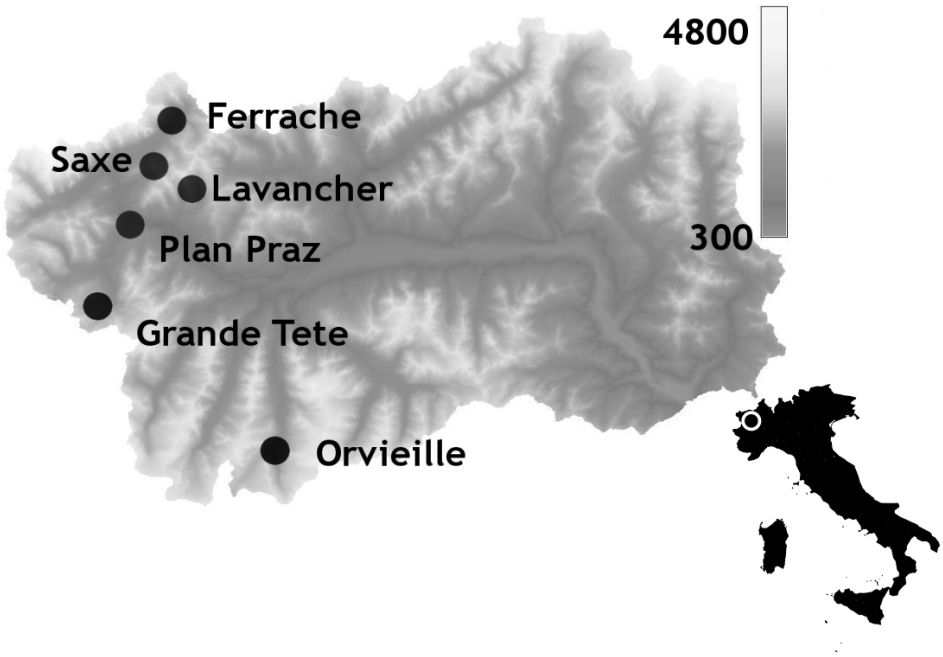

Figure 1: Location of the study sites. Dots represent AWS used in this study. The grey scale in the upper-right panel represents elevation (m ASL).

Table 1: Main characteristics of the 6 study sites.

	Long (°)	Lat (°)	Elevation (m)	Period
Ferrache	7.02	45.86	2290	2001-2009
Saxe	6.98	45.81	2076	1992-2009
Grande Tête	6.91	45.68	2430	1998-2009
Lavancher	7.02	45.80	2842	1992-2009
Plan Praz	6.95	45.76	2044	1999-2009
Orvieille	7.19	45.58	2170	2005-2009

2.2. Data collection

Aosta Valley's meteorological network consists of 91 AWS. Beside measuring the classical meteorological parameters (such as precipitation, T_{air}, wind speed and direction), 40 AWS also measure snow depth and six measure snow temperatures (T_{snow}). In this work we analyzed the data recorded by these six AWS (Fig.1, Tab.1). T_{snow} was measured at 20 cm increments between 0 and 400 cm from the soil surface with a sampling frequency of 4 hours. The array of the T_{snow} sensors is mounted on a white-painted, 4-m-height mast, located few meters apart from AWS.

Each weather station recorded snow depth by means of snow sensors, shielded T_{air}, barometric pressure, wind speed and direction at 30-min intervals. Total radiation was measured at the same intervals in 5 of the 6 AWS, since one of them (Orvieille) was not equipped with the radiometer. Published accuracies for the snow depth sensors and the termometers were 1 cm and 0.2 °C, respectively. All instruments have been manufactured and installed

by CAE (Bologna, Italy), and operated and maintained by Centro Funzionale Regionale, Regione Autonoma Valle d'Aosta.

2.3. Data processing

Data quality check is pivotal for automatically-operated, only periodically-maintained sensors, such the ones we have analyzed. A first quality check was done in order to detect data affected by wrong acquisition, i.e. erroneous data, most commonly a constant series of -30 °C readings for a long period. This was done by quantitatively evaluating the relationship between T_{snow} and T_{air} data. We first calculated the difference between T_{air} and T_{snow} at each level. We then applied a threshold on the difference of -20 and +30 °C respectively and removed all data falling outside that interval. The temperature thresholds are not physically based but were set arbitrarily after an exploratory analysis. Hence, since we cannot *a priori* exclude that real data may have been removed, the temperature gradient analysis was also run on the unfiltered dataset, with the same results, indicating that even if real temperature records may have been removed, these data were probably for the snow free period or for heights above the snowpack. Based on that analysis, a small number of records (about 3% of the total) was removed.

One major issue in the dataset was detected in springtime data. When the snow melts, the mast (although white painted) conducts much heat and allows the surrounding snow to melt faster than it would occur under natural conditions. This occurrence results in free space around the sensors similar to that found around tree stems during snowmelt. In terms of measured temperatures, this resulted in positive temperatures at heights that were supposed to be inside the snowpack. A careful analysis showed that this feature

occurred systematically each spring at all sites and across all depths. We therefore decided to assume that all positive temperatures occurring within the snowpack were indicative of a melting snowpack, and substituted all positive temperatures with 0 °C values. By this procedure an average across all sites of 30% data were replaced. This substantial data filling was necessary in order to get reliable snow temperature profiles and subsequent temperature gradients. In the results section we will show how this correction affected the computation of temperature gradients.

A second issue was represented by drifts in the sensors. Thermometers were calibrated by the manufacturer before installation, but after that any further inter-calibration was not performed or, if performed by manufacturer, it was not tracked. To check the inter-comparability of temperatures measured at different heights within one site we performed the following analysis. From the complete 4-hour time series of a given site we selected snow-free (HS=0 cm), nighttime (total radiation less than 20 W m^{-2}, Papale et al. (2006)) data in order to exclude the effect of solar radiation. We then further subset the data to get a sample of well mixed atmospheric conditions (wind speed higher than 0.5 m s^{-1}), i.e. when the air column on the whole 4-m array is well mixed and therefore unlikely to show air stratification and consequently a temperature gradient. For each temperature profile we calculated the deviation from the profile mean and used a contour plot analysis to show shifts in the sensors that could be caused by drifts.

Fig.2 shows one example of this analysis (about 2000 profiles from site Grande Tête). A consistent departure from the mean temperature profile at a given height (as at 200 cm in fig.2) may represent a drift in the sensor measure-

ment. However, those drifts are not consistent through the whole period, probably due to a manufacturer's recalibration of the sensors that was not tracked by the operators. To take into account this source of uncertainty we applied two different filters.

(1) For each 4-hour vertical temperature profile we computed the difference in temperature from each adjacent sensor. If this difference was higher than 10 °C (i.e., leading to a temperature gradient of 50 °C/m or higher), the record was discarded. Discarded data were then gap-filled by linear interpolation. The 50 °C/m threshold was chosen according to published values of partial gradients (Hood et al., 2005; Birkeland, 1998). These studies report near-surface temperature gradients much higher than 50 °C/m only very close to the snow surface and at very small vertical increments (e.g. 5 cm increments). The magnitude of those surface gradient decrease exponentially with depth, so that at 15-20 cm from the snow surface values of partial gradient exceeding 50 °C/m were not reported. Based on these values, and given the relatively coarse vertical resolution of our thermistor array we assume that values higher than 50 °C/m can hardly be measured by our experimental setup.

(2) For each vertical temperature profile, we first increased the resolution from 20 to 0.2 cm, by linearly interpolating (using a cubic spline) between points. We then computed a moving average with a 40 cm resolution window resulting in smoothed, reconstructed temperature profiles in the snowpack. The drift analysis was then performed on the filtered datasets, and resulted in a general increase in data quality (Fig. 2). In the result section we will show how this correction affect the computation of temperature gradients in

189 the snowpack.

190

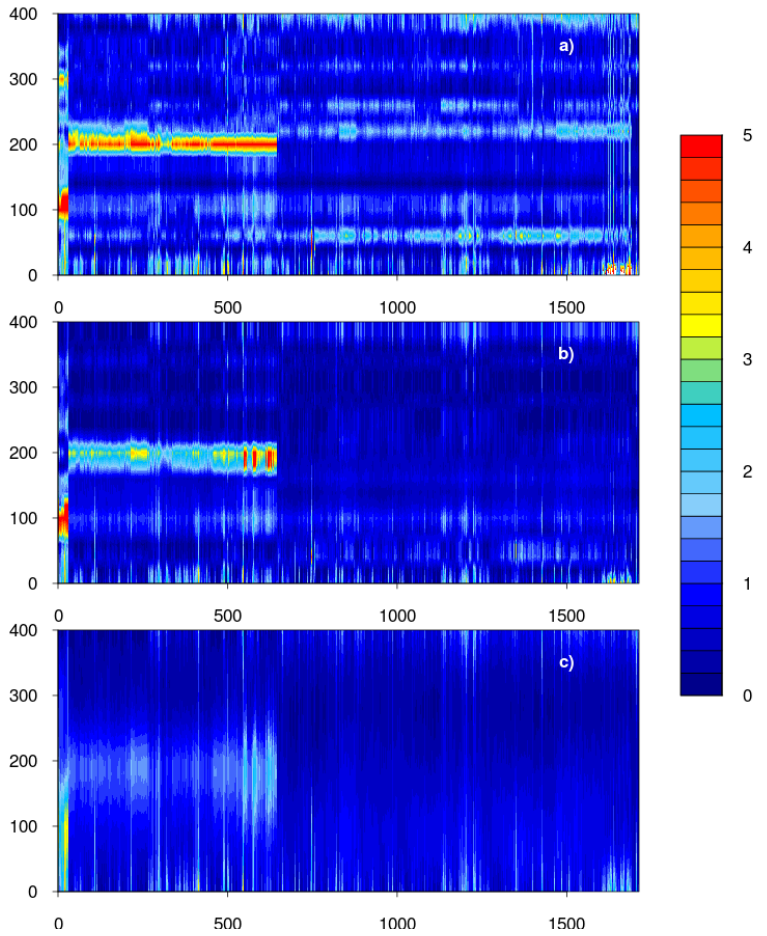

Figure 2: Contour plot of absolute deviations from the mean temperature profile (°C) showing potential drifts in the sensors for site Grande Tête for PST dataset (a), DA dataset (b), and MAA dataset (c). To stretch values in the low range, values higher than 5 °C were set at 5 °C

191 In summary, the three filtering steps lead to four different datasets: (1)
192 unfiltered data (RAW), (2) data filtered for positive T_{snow} (PST), (3) data

filtered for drifts with the Difference Approach (DA), and (4) data filtered for drifts with the Moving Average Approach (MAA).

2.4. Temperature gradient analysis

The snow temperature gradients (°C/m) were computed as the difference in temperature between the lower of two adjacent thermistors and the upper one divided by the vertical distance (0.20 m). A partial gradient is considered within the snowpack when the upper thermometer is covered by at least 10 cm of snow.

For some of the analyzes that we will present, among the whole array of partial gradients in the snowpack, we focused on two remarkable ones: the basal gradient (BG, calculated between 0 and 20 cm), and the surface gradient (SG, the gradient calculated approximately at the snow surface). The basal gradient is of interest to investigate the occurrence of depth hoar, whereas the surface gradient for near-surface faceted crystals.

In order to test the possibility to predict temperature gradients based on environmental parameters, we investigated the relationship between BG, SG and snow depth, T_{air}, solar radiation, and wind speed.

All data have been analyzed using R software for statistical computing (R development core team, 2010).

3. Results

Main characteristics of the study sites for the measurement period are reported in table 1, and basic meteorological data are represented in Fig. 3.

T_{air} exhibits a linear decrease with elevation, with Lavancher (2842 m a.s.l.) being the coldest site. Average monthly snow depths are consistently higher in Saxe and Lavancher. The latter shows furthermore a different timing in the seasonal distribution of the snowpack, with delayed snowmelt compared to other sites, as a consequence of higher elevation.

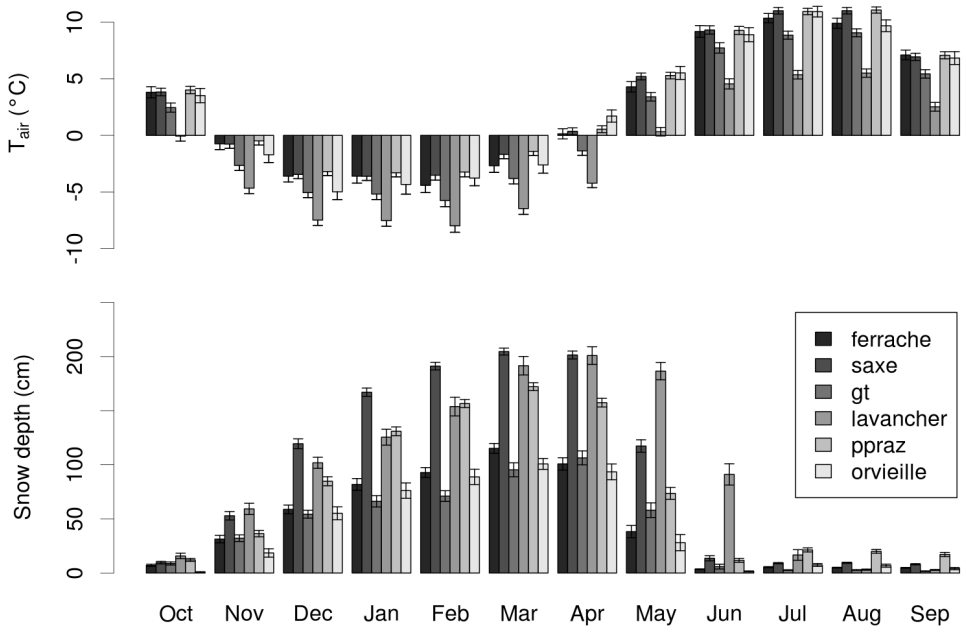

Figure 3: Monthly average air temperatures and snow depths at the six investigated sites. Error bars represent confidence intervals.

3.1. Snow temperatures

The seasonal course of vertical profiles of T_{snow} are shown by means of contour plots (Fig.4). The depth of the snowpack affects snow temperatures during the course of the winter. While episodic cold periods and the resulting low air temperatures can lower snow temperature close to the surface (as in

the period from January to March in Fig.4, when minimum recorded T_{snow} were close to -20 °C), snow temperature at the snow/soil interface remains close to 0 °C for the whole winter (Pomeroy and Brun, 2000). Starting from the beginning of April, the melting snowpack becomes consistently isothermal.

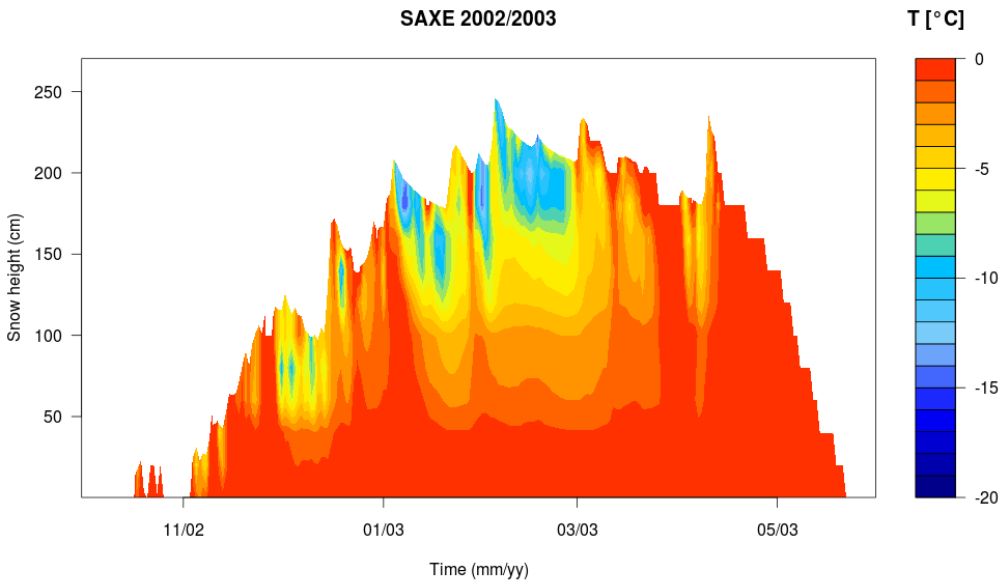

Figure 4: Seasonal course of mean daily snow temperatures for Saxe in winter 2002-2003. Dataset: PST.

Fig.4 reports an example of relatively warm and deep snowpack occurring in a warm winter. To illustrate the behavior of snow thermal properties in a cold and less snowy winter (e.g. 2004-2005), we show the contour plot of the site located at highest elevation (Lavancher, Fig.5). A long period of cold air temperatures in the period from mid February to mid March results in a cold

front in a relatively shallow snowpack that penetrates down to the snow/soil interface. Note that at the end of the cold period, the snowpack gradually warms from the surface, driven by higher air temperatures, whereas at the snow/soil interface temperature remains lower, resulting in a negative surface gradient.

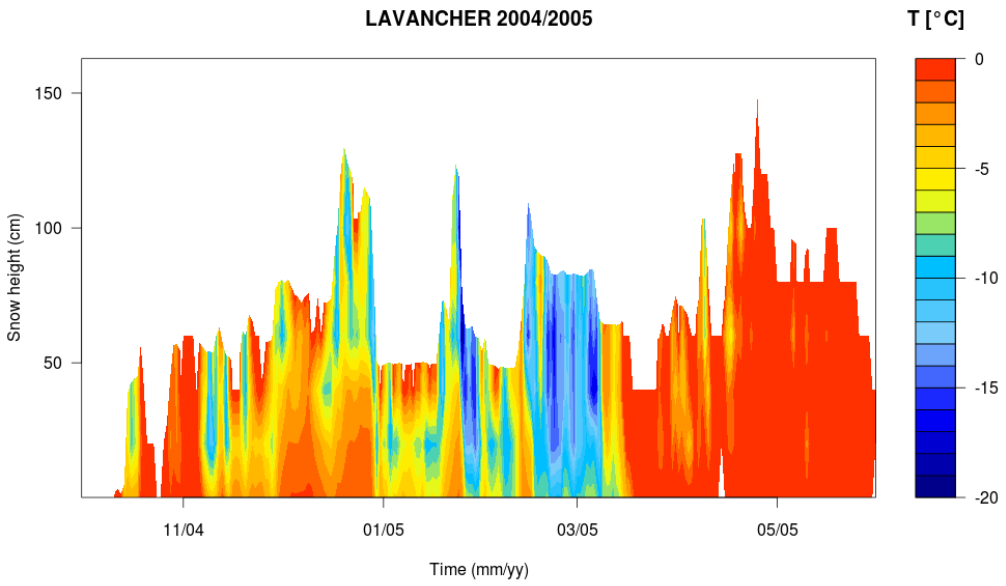

Figure 5: Seasonal course of daily snow temperatures for Lavancher in winter 2004-2005. Dataset: PST.

3.2. Temperature gradients

Fig. 6 shows an example of seasonal course of hourly partial gradients in the snowpack.

At this site, positive gradients in the snowpack occur throughout winter and early spring. Strong positive gradients at the snow surface between February

and March coexist with lower positive gradients in the lower portion of the snowpack. At the snow surface, the diurnal alternation between positive and negative gradients is evident.

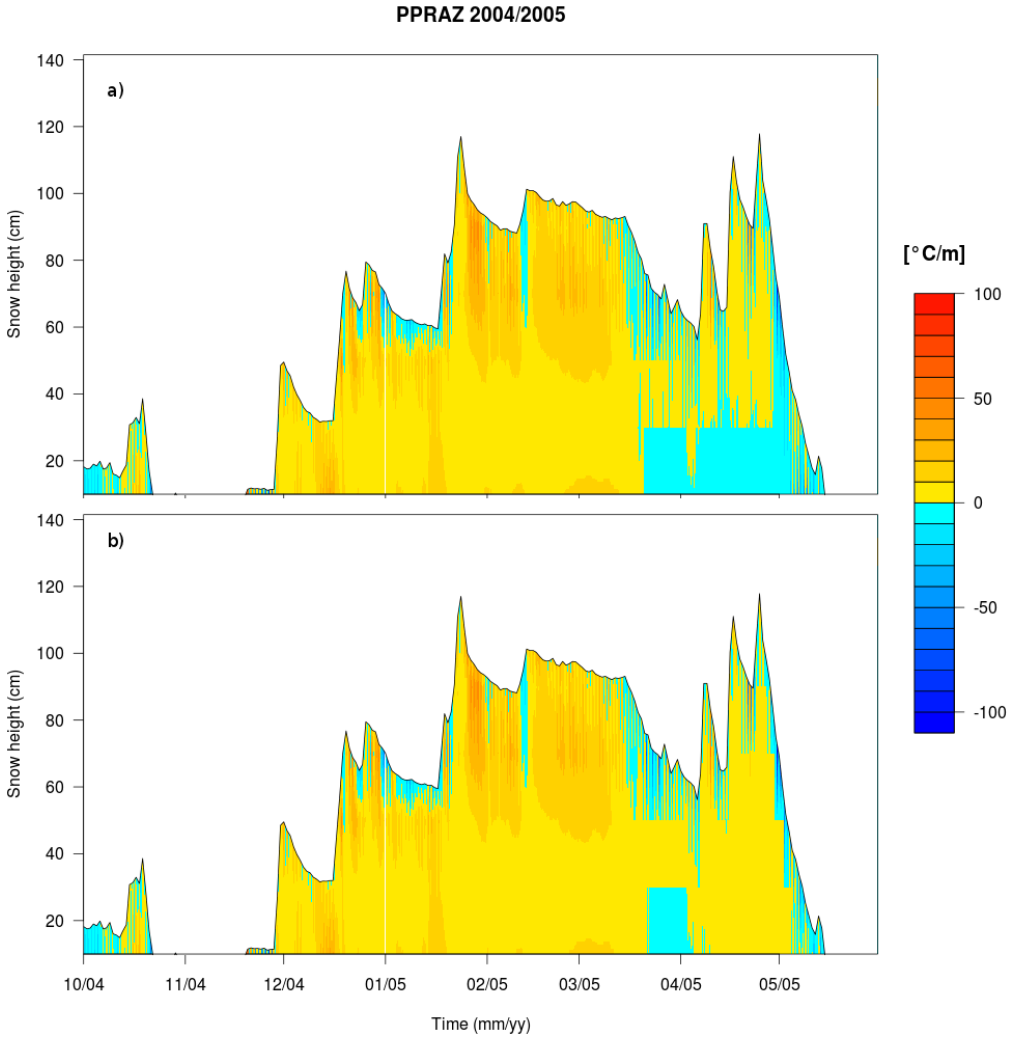

Figure 6: Seasonal course of hourly partial gradients for Plan Praz in winter 2004-2005. The black solid line depicts snow depth. a) RAW dataset, b) PST dataset.

Fig. 6b shows data corrected for positive spring temperatures, whereas Fig. 6a shows the same data uncorrected. Negative gradients at the base of the snowpack in spring are an artifact due to the unrealistic above-zero temperatures in the snowpack.

3.3. Strong temperature gradients in the snowpack: occurrence and duration

Particularly relevant to snowpack stability are temperature gradients higher than 20 °C/m. The 4-hour dataset was used to compute the relative number of weak (<5 °C/m), medium (between 5 and 20 °C/m) and strong (>20 °C/m) gradients. Gradients were taken as absolute values for this analysis, because heat fluxes may be responsible for constructive metamorphism both upwards and downwards. Fig. 7 reports the frequency histograms for basal gradient (BG) and surface gradient (SG), averaged across all sites and separated for the three datasets, computed over the entire study period. There is a common pattern across all datasets and snowpack portions, with generally more than 60% of gradients being classified as weak, and a decreasing occurrence of medium and strong gradients. The frequency of strong gradients is significantly higher in SG compared to BG for all datasets. Correspondingly, the frequency of weak gradients is significantly lower in SG compared to BD. Comparing the different datasets, the highest number of strong gradients was found in the unfiltered dataset (RAW, Fig. 7a). Data filtered for positive T_{snow} (PST) feature a higher number of weak gradients and a lower number of medium gradients compared to RAW, with no difference on strong gradients. The effect of the difference-approach filtering (DA) was very similar to that of PST. The moving-average-approach (MAA) resulted in an increase in weak gradients, and in a decrease in both medium and

strong gradients compared to RAW data. To give an estimate of the relative number of negative and positive temperature gradients, these were computed on the DA dataset for surface gradients (the gradients that are expected to show the largest number of negative gradients). Averaged across all sites positive strong gradients were about 80% of total strong gradients.

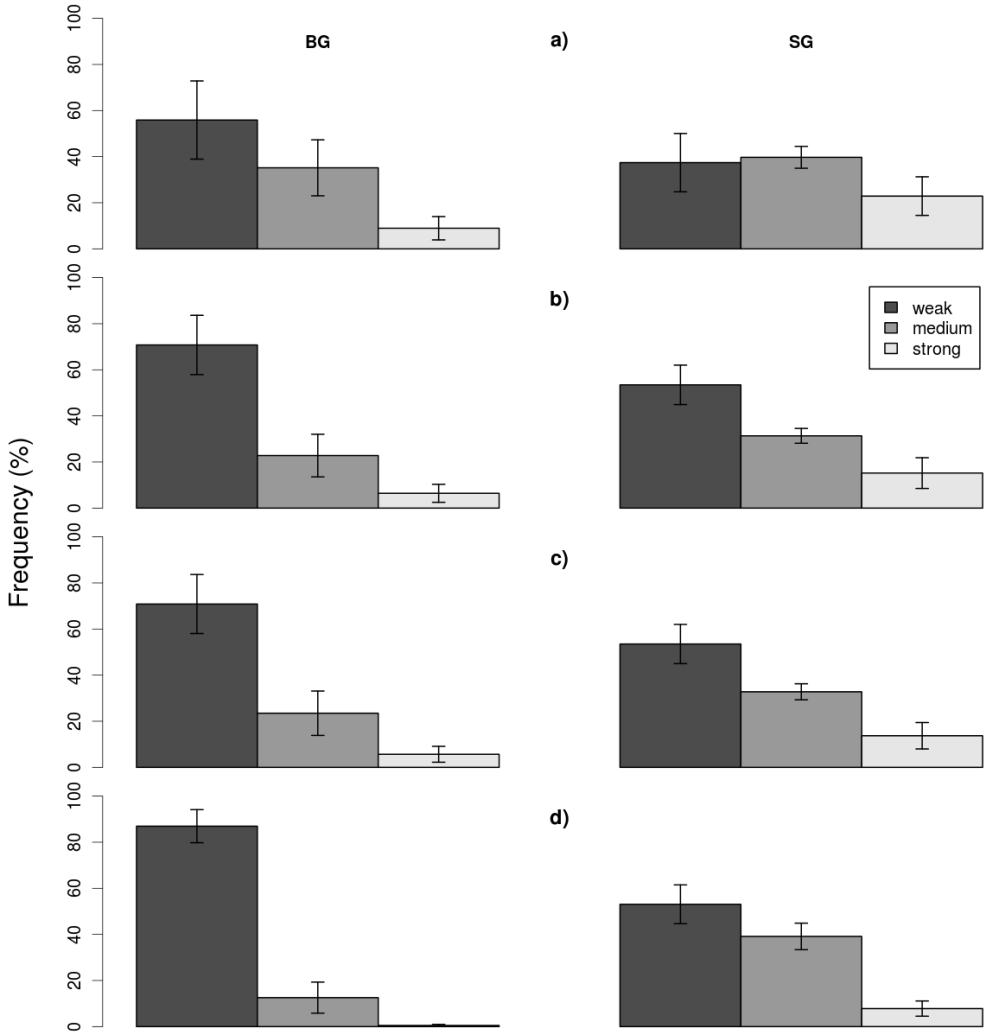

Figure 7: Relative number of temperature gradients according to classes weak, medium and strong in two portions of the snowpack (BG, basal gradient; SG, surface gradient), for the raw data (a, RAW), the data filtered for positive T_{snow} (b, PST), data filtered for drifts using the difference approach (c, DA), and data filtered for drifts using the moving average approach (d, MAA).

Table 2 reports the relative number of strong partial gradients at the

base of the snowpack for each site, according to different filters applied. As shown also in Fig. 7 strong gradients decrease from RAW to highly filtered data at all sites, even if strong differences exist across sites. This difference is associated to the different snow patterns of those sites, in particular Ferrache, Grande Tête and Orvieille show lower snow depths compared to Lavancher, Saxe and Plan Praz. Instead, surface temperature gradients appear to be positively related to elevation (cfr. Table 1).

Table 2: Relative number (%) of strong partial gradients at the base of the snowpack and at the snow surface for each site according to the different filters applied.

	BG				SG			
Site	RAW	PST	DA	MAA	RAW	PST	DA	MAA
Ferrache	16.7	8.5	7.1	0.5	27.9	14.3	13.3	5.9
Saxe	1.5	1.1	1.0	0.1	16.9	10.0	9.6	6.7
Grande Tête	10.9	9.1	7.3	0.4	36.7	27.5	23.5	14.4
Lavancher	7.3	4.5	4.3	0.2	23.8	12.6	11.6	7.0
Plan Praz	2.4	1.7	1.6	0.1	6.0	4.5	4.0	2.4
Orvieille	14.8	13.7	12.6	1.6	26.0	22.1	20.3	10.5

To evaluate the duration of strong gradients in the snowpack, we calculated the number of consecutive days with strong gradients, and for each site we computed the maximum number of consecutive days with strong gradients (Table 3). For this analysis, we used the daily partial gradients (absolute values). The maximum number of consecutive days was found at site Grande Tête in the RAW dataset, with as much a 154 consecutive days with a temperature gradient higher than 20 °C/m. In general, there is a good agreement

between dataset PST and DA, except for Ferrache and Grande Tête. RAW data lead to highest number of consecutive days with strong gradients for all sites except Ferrache, whereas the MAA filtering procedure always resulted in the lowest number of consecutive days.

For sites Plan Praz and Orvieille the highest number of consecutive days was consistently found at the snow surface for all datasets. The mean duration (in days) of a persistent strong gradient (all depths mediated) was fairly constant across sites and datasets, ranging between 1 and 2.5 days, except for site Grande Tête in RAW dataset, which was much higher.

Table 3: Average(±SD) and maximum number of consecutive days with mean daily gradient higher than 20 °C/m for all sites and all datasets. For maximum, depth and year of occurrence are also indicated.

Site	Dataset	N days (mean)	N days (max)	Depth (max)	Year (max)
Ferrache	RAW	1.9±0.8	21	40-60 cm	2009
	PST	1.9±0.7	23	0-20 cm	2005
	DA	1.6±0.5	14	60-80 cm	2009
	MAA	1.1±0.3	5	60-80 cm	2009
Saxe	RAW	1.6±0.5	12	0-20 cm	1999
	PST	1.5±0.5	12	0-20 cm	1999
	DA	1.4±0.4	12	0-20 cm	1999
	MAA	1.2±0.3	5	100-120 cm	2005
Grande Tête	RAW	8.1±14.1	154	80-100 cm	2001
	PST	1.9±1.5	21	Surface	2001
	DA	1.6±1.0	16	0-20 cm	2006
	MAA	2.4±3.0	5	0-20 cm	2006
Lavancher	RAW	2.3±1.4	117	40-60 cm	2008
	PST	2.0±0.9	35	40-60 cm	2008
	DA	2.0±0.7	35	40-60 cm	2008
	MAA	1.3±0.6	8	Surface	2007
Plan Praz	RAW	1.6±0.6	8	Surface	1999
	PST	1.7±0.8	8	Surface	1998
	DA	1.7±0.7	8	Surface	1998
	MAA	1.4±0.6	5	Surface	2005
Orvieille	RAW	1.9±1.4	15	Surface	2005
	PST	2.0±1.5	15	Surface	2006
	DA	2.0±1.4	15	Surface	2006
	MAA	1.1±0.1	2	Surface	2006

3.4. Relationship between temperature gradients and environmental variables

We hypothesized a strong relationship between snow depth, T_{air} and the snow temperature gradients. As an example, this relationship is illustrated in Fig. 8 for 4-hour partial gradients from the PST dataset. As expected, absolute values of partial gradients at the base of the snowpack are higher with lower snow depths and gradually get closer to 0 °C/m with increasing snow depth. The same pattern can be seen at the surface, but with increasing scatter, suggesting that other factors exert a major influence at the snow surface.

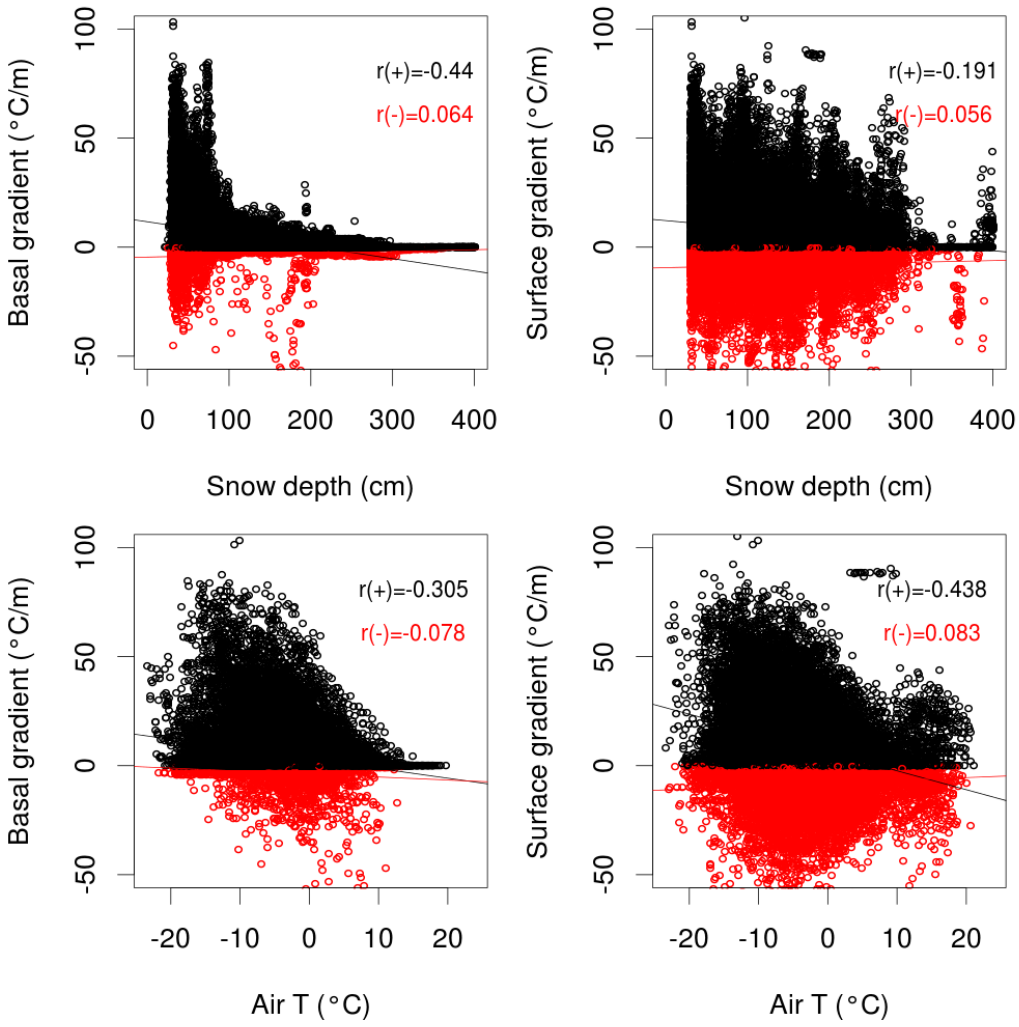

Figure 8: Scatter plot between hourly partial gradients (positive in black, negative in red), air temperature and snow depth, for all sites and years, dataset: PST.

Table 4: Pearson correlation coefficient between snow temperature gradients (separated between positive and negative gradients, column 'sign'), snow depth and air temperature for different datasets (all coefficients are significant at $p<0.001$, except those denoted by *).

Gradient	Dataset	Sign	Snow depth	T_{air}	Total radiation	Wind speed
BG	RAW	+	-0.33	-0.14	-0.03	-0.09
		-	0.25	-0.24	-0.23	0.00*
SG		+	-0.18	-0.27	0.05	-0.03
		-	0.07	-0.15	-0.36	0.05
BG	PST	+	-0.44	-0.30	-0.12	-0.10
		-	0.06	-0.08	-0.10	-0.09
SG		+	-0.19	-0.44	-0.14	-0.03
		-	0.06	0.08	-0.16	0.09
BG	DA	+	-0.47	-0.31	-0.13	-0.10
		-	0.16	-0.06	-0.12	-0.10
SG		+	-0.18	-0.45	-0.16	-0.02
		-	0.06	0.10	-0.15	0.09
BG	MAA	+	-0.46	-0.34	-0.13	-0.12
		-	0.42	-0.16	-0.14	0.03
SG		+	-0.08	-0.38	-0.03	-0.01*
		-	-0.01*	-0.19	-0.30	0.00*

Table 4 reports the correlation coefficients between snow temperature gradients and relevant environmental variables. Higher correlations were found between gradients, snow depth and T_{air}, whereas the relationship between gradients, solar radiation and wind speed was weaker. PST and DA filtering improves the correlation between either basal and surface positive tempera-

ture gradients, and snow depth and T_{air}, whereas MAA filtering results in lower correlation between gradients and snow depth, but higher correlation with T_{air}. The relatively weak relationship between partial gradients, snow depth and T_{air} suggests that partial gradients cannot be predicted by means of such simple environmental drivers. We performed a multiple regression with T_{air} and snow depth as regressors and partial gradients (positive and negative gradients separated) at all depths and found that none of them could be properly predicted using any datasets. We furthermore tried to include other environmental data (solar radiation, wind speed, air pressure, etc.) as regressors when available, but with no substantial improve of the model (data not shown). Multiple regression models showed R^2 always lower than 0.4. The pattern of R^2s across different datasets reflected the pattern of correlation coefficients shown in table 4.

4. Discussion

4.1. The effect of data filtering on temperature gradient computation

An extensive dataset (67 site-years) of continuous measurements of T_{snow} represents an invaluable tool to evaluate the occurrence and the duration of strong temperature gradients at relatively small stratigraphic scale in the snowpack. However, we have identified 3 sources of uncertainty on the data that must be taken into account to get reliable information. Uncertainties include erroneous data, positive T_{snow} in spring and drifts in the thermistors. Erroneous data were removed by evaluating the relationship between T_{snow} and T_{air}, and this correction did not affect the computation of snow temperature gradients. However, thresholds in this analysis were arbitrarily

chosen and dataset-specific. Therefore, they should be applied with caution on other datasets.

Approximately 30% of positive temperatures in the snowpack were removed and substituted by 0 °C. This correction resulted in more realistic temperature gradients in the snowpack in spring (cfr. Fig. 6). The relative number of gradient classes was also affected by the filtering as shown in Fig. 7. The second filtering (DA) was intended to remove large sensors drifts, and showed very similar results compared to PST. The MMA filtering was intended to remove small drifts in the vertical temperature profile and resulted in a general smoothing of the partial gradients. Consequently, compared to RAW and PST datasets, this filtering produced a higher number of weak gradients, and a lower number of medium and strong gradients. The smoothing effect of filtering was reflected also in the computation of consecutive days with strong gradients (Table 3), with a decrease in duration towards subsequent filtering steps. The unrealistic number of maximum consecutive days with strong gradients calculated in Lavancher and Grande Tête in the RAW dataset is associated to positive T_{snow} and the difference between unfiltered and filtered data in this analysis demonstrates the usefulness of PST filter. Instead, the small difference found between PST and DA filtering suggests that this latter correction only marginally affects the gradient calculation, even if DA filter was effective in reducing the effect of sensor drifts (cfr. Fig 2). Since the difference between PST and DA filtering is small, we also confirm our preliminary assumption that gradients higher than 50 °C/m can hardly be measured by this experimental setup.

MAA filtering strongly reduces the occurrence and duration of strong gra-

dients, and fails in identifying inter-site differences in temperature gradients (discussed later). This is because MAA filtering resulted in an inordinate smoothing of temperature vertical profiles that in turn possibly lead to an underestimation of strong temperature gradients.

In summary, the combination of PST and DA filters significantly improves the dataset and may be applied to similar experimental setup. However, it must be noted that the gradient threshold of 50 °C/m should likely be increased in case of gradients measured at depth increments smaller than those used in this study (20 cm). In fact, gradients larger than 50 °C/m were reported by previous studies in small portions of the snowpack surface at 5 to 10 cm increments (Hood et al., 2005; Birkeland, 1998; Greene et al., 2006).

4.2. Magnitude of snow temperature gradients and variability across sites

Snowpack instability due to constructive metamorphism is usually associated to strong temperature gradients at the base of the snowpack and the formation of depth hoar. However, strong surface gradients may promote the formation of near-surface faceted crystals, which, if buried by new snow, might also result in potential snowpack instability (Birkeland, 1998; Hood et al., 2005). Here we show that the occurrence of strong temperature gradients is significantly higher at the snow surface than at the snowpack base (Fig. 7), highlighting the importance of considering surface snow properties for snowpack stability.

Based on DA dataset we estimated that strong temperature gradients (i.e absolute gradients higher than 20 °C/m) account for between 1 and 13% of total gradients at the base of the snowpack, and for between 4 and 24% at

the snow surface. With respect to snowpack stability, the first are associated to full-depth avalanches, whereas the latter to surface slab avalanches, often human-triggered (Schweizer and Jamieson, 2001; Schweizer and Lütschg, 2001). The mean duration of strong temperature gradients ranged from 1.4 to 2 days, whereas the maximum duration varied across sites from 8 to 35 days. These time interval is sufficient for the development of faceted crystals that might result in persistent weak layer (Birkeland, 1998). In two out of six sites these long-lasting strong temperature gradients occurred at the snow surface, whereas in two sites they occurred at the bottom of the snowpack. These extreme gradients are not related to a specific, particularly cold or snow-poor winter.

05 Although a strong relationship between snow depth, T_{air} and snow temperature gradients was not found, the occurrence and duration of these varied across sites, primarily as a function of environmental drivers. The relative number of strong partial gradients at the base of the snowpack reported in table 2 was higher in Ferrache, Grande Tête and Orvieille, which are also the sites characterized by lower snow depths (Fig. 3), and lower in Lavancher and Saxe. This pattern can be seen for all datasets, but only for PST the correlation between the relative number of strong gradients and the mean snow depth was significant ($r=-0.849$, $p<0.05$). A similar behavior is also apparent for the duration of strong gradients (Table 3). Surface gradients are less correlated with T_{air} and appear to be instead related to elevation. Elevation is in turn related to solar radiation (positively) and to T_{air} (negatively) and may therefore be seen as a number that integrates the two. However, no direct relationship was found between occurrence or duration of surface

gradients and radiation or T_{air}.

Even if in some cases synthesis data such as relative number and maximum duration of strong gradients showed a relationship with snow depth, T_{air} and elevation, the lack of such a clear relationship for 4-hourly and daily temperature gradients prevented us from modeling the seasonal course of temperature gradients based on simple environmental parameters.

5. Conclusions

The analysis of a large dataset of snow temperature profiles (about 3 millions temperature records, from 67 site-years) has shown important features related to the measurement of snow temperatures and the calculation of temperature gradient in the snowpack but also highlighted a number of issues related to data quality. Data quality check has allowed to: (1) remove about 3% of the data likely associated with errors in the data logging; (2) identify a substantial problem related to melting snow around the sensors during spring which leads to positive snow temperatures; in order to solve this problem we had to replace about 30% of fake, positive snow temperatures, assuming that temperature was 0 °C; and (3) identify a procedure based on the analysis of snow-free, nighttime temperature profiles that allowed to identify drifts in the sensors, corrected by means of two subsequent filtering procedures (DA and MAA).

Filtering for (1) did not affect the snow gradient computation, whereas filtering for (2) substantially improved the data quality and the reliability of calculated snow temperature gradients. With respect to (3), DA filtering resulted in a small improvement of data, whereas MAA resulted in an inordi-

nate smoothing of temperature vertical profiles that in turn possibly lead to an underestimation of strong temperature gradients. Reliable snow temperature datasets may therefore be obtained by applying a filter for above zero snow temperatures and a threshold for unrealistically high partial gradients. This threshold must however be adjusted based on the vertical resolution of temperature measurements.

Based on this extensive dataset, we estimated that strong temperature gradients may account for as much as 25% of total gradients and the duration of these may be as long as 35 days. The frequency of strong gradients is significantly higher at the snow surface than at the snowpack base. Therefore the formation of near-surface faceted crystals as potential weak layers must be taken into account when assessing snow stability in alpine snowpack.

6. Acknowledgments

This research was founded in the framework of the *Incarico di collaborazione per l'elaborazione dei dati di temperatura del manto nevoso raccolti dalle stazioni nivometeorologiche automatiche gestite dal Centro Funzionale della Valle d'Aosta, nell'ambito del P.O. di Cooperazione territoriale europea transfrontaliera Italia/Francia (Alpi) 2007/2013 ALCOTRA - Progetto RiskNat Gestione in sicurezza dei territori di montagna transfrontalieri.*

We are grateful to Dr. Eric Lutz for his thorough review, which substantially improved the quality of this work.

References

Adams, E.E., Brown, R.L., 1983. Metamorphism of dry snow as a result of temperature gradient and vapor density differences. Ann. Glaciol. 4, 3-9.

Bakermans L.A., Jamieson J.B., 2006. Measuring near-surface snow temperature changes over terrain. Proceedings ISSW 2006. International Snow Science Workshop,Telluride CO, U.S.A., 1-6 October 2006, 377-386.

Bartelt P., Lehning M., 2002. A physical SNOWPACK model for Avalanche Warning Services. Part I: numerical model, Cold Reg. Sci.Technol. 35, 123-145.

Beniston M., Uhlmann B., Goyettea S., Lopez-Moreno J.L., 2010. Will snow-abundant winters still exist in the Swiss Alps in an enhanced greenhouse climate? Int. J. Climatol. 31 (9), 1257-1263.

Birkeland K.W., 1998. Terminology and predominant processes associated with the formation of weak layers of near-surface crystals in the mountain snowpack. Arctic and Alpine Research, 30(2), 193-199.

Brun E., Martin E., Simon V., Gendre, C., Coleou, C., 1989. An energy and mass model of snowcover suitable for operational avalanche forecasting, J. Glaciol. 35, 333-342.

Colbeck, S.C., 1983. Theory of metamorphism of dry snow. J. Geophys. Res., 88(C9), 5475-5482, doi:10.1029/JC088iC09p05475.

Colbeck, S.C., Jamieson, J.B., 2001. The formation of faceted layer above crusts. Cold Reg. Sci.Technol. 33, 247-252.

Fierz C., 2011. Temperature profile of snowpack. In: Encyclopedia of Snow, Ice and Glaciers (ed. Singh, V.P., Singh, P., and Haritashya, U.K.), Springer, Netherlands, 1151-1154.

Fierz C., Bakermans L.A., Jamieson J.B., Lehning, M., 2008. Modeling short wave radiation penetration into snowpack: What can we learn from near-surface snow temperatures? Proceedings ISSW 2008. International Snow Science Workshop, Whistler, BC, CAN, 21-27 September, 2008, 204-208.

Giddings, J. C., LaChapelle, E., 1962. The formation rate of depth hoar, J. Geophys. Res., 67(6), 2377-2383, doi:10.1029/JZ067i006p02377.

Gray D. M., Male D.H. (eds.), 1981. Handbook of snow: Principles, processes, management and use: Toronto, Ontario, Pergamon Press.

Greene E.M., Schneebeli M., Elder K., 2006. The microstructual effects of kinetic growth metamorphism in a layered snow structure. International Snow Science Workshop 2006 Proceedings, ISSW 2006, Telluride, Colorado.

Hood E., Scheler K., Carter P., 2005. Near-surface faceted crystals formation and snow stability in a highh-latitude maritime snow climate, Juneau, Alask

Jones H.G., Pomeroy J.W., Walker, D. A., and Hoham, R. W. (eds.), 2001. Snow Ecology: An Interdisciplinary Examination of Snow-Covered Ecosystems. Cambridge: Cambridge University Press.

Jordan R., 1991. A one-dimensional temperature model for a snowcover. CRREL Spec. Rep. 91-16.

Kaempfer T.U., Schneebeli M., and Sokratov S.A., 2005. A microstructural approach to model heat transfer in snow. Geophysical Research Letters, 32(21), L21503, doi:10.1029/2005GL023873.

Lehning M., Bartelt P., Brown R.L., Russi T., Stoeckli U., Zimmerli M., 1999. SNOWPACK model calculations for avalanche warning based upon a new network of weather and snow stations. Cold Reg. Sci. Technol. 30, 145- 157.

Lehning M., Bartelt P., Brown R.L., Fierz C., Satyawali P.K., 2002a. A physical SNOWPACK model for the Swiss avalanche warning Services; Part II. Snow microstructure. Cold Reg. Sci.Technol. 35(3), 147-167.

Lehning M., Bartelt P., Brown R.L., Fierz C., 2002b. A physical SNOWPACK model for the Swiss avalanche warning Services; Part III: meteorological forcing, thin layer formation and evaluation. Cold Reg. Sci. Technol. 35(3), 169-184.

Marienthal A., Hendrikx J., Chabot D., Maleski P., and Birkeland K., 2012. Depth hoar, avalanches, and wet slabs: A case study of the historic March, 2012 wet slab avalanche cycle at Bridger Bowl, Montana. Proceedings of the 2012 International Snow Science Workshop, Anchorage, AK.

McClung D., Schaerer P., 2006. The Avalanche Handbook, The Mountaineers Books. 342 pp.

Mercalli L., Castellano C., Cat Berro D., Di Napoli, G., 2003. Atlante Climatico della Valle d'Aosta. (Climate Atlas for the Aosta Valley Region) (SocietÃă Meteorologica Subalpina).

Morland L.W., Kelly R.J., Morris E.M., 1990. A mixture theory for a phase-changing snowpack. Cold Reg. Sci. Technol. 17, 271- 285.

Ohara N., Kavvas M.L., 2006. Field observations and numerical model experiments for the snowmelt process at a ïňĄeld site. Advances in Water Resources, 29, 194-211.

Papale D., Reichstein M., Aubinet M.E., Canfora E., Bernhofer C., Kutsch W., Longdoz B., Rambal S., Valentini R., Vesala T., et al.(2006), Towards a standardized processing of Net Ecosystem Exchange measured with eddy covariance technique: algorithms and uncertainty estimation, Biogeosciences, 3(4), 571-583.

Pomeroy J.W., Brun E., 2000. Physical properties of snow. In: Snow Ecology, Cambridge University Press pp. 378.

R Development Core Team, 2010. R: A language and environment for statistical computing. R Foundation for Statistical Computing, Vienna, Austria. ISBN 3-900051-07-0, URL http://www.R-project.org/.

Reusser D.E., Zehe E., 2011. Low-cost monitoring of snow height and thermal properties with inexpensive temperature sensors. Hydrol. Process. 25, 1841- 1852.

Shea C., Jamieson B., Birkeland K.W., 2012. Use of a thermal imager for snow pit temperatures. The Cryosphere, 6, 287-299.

Schweizer J., Jamieson J.B., 2001. Snow cover properties for skier triggering of avalanches. Cold Reg. Sci. Technol. 33 (2-3): 207-221.

556 Schweizer J., Lütschg M., 2001. Characteristics of human-triggered
557 avalanches. Cold Reg. Sci. Technol. 33 (2-3): 147-162.